Phospholipid-independent biogenesis of a functional RP4 conjugation pilus

Naito Ishimoto[1,2,#], Gad Frankel[1,*], Konstantinos Beis[1,2,*]

Running title: Lipid-independent biogenesis of the RP4 pilus

[1]Department of Life Sciences, Imperial College London, London SW7 2AZ, UK

[2]Rutherford Appleton Laboratory, Research Complex at Harwell, Didcot, Oxfordshire, OX11 0FA, UK

[#]current address: Drug Design Laboratory, Graduate School of Medical Life Science, Yokohama City University, Tsurumi, Yokohama, 230-0045, Japan

Keywords: conjugative pilus; mating pair formation; cyclization; lipid-independent pilus biogenesis; phospholipids

[*]corresponding authors: g.frankel@imperial.ac.uk and kbeis@imperial.ac.uk

Abstract

Conjugation of the RP4 plasmid is mediated by short, non-retractable, rigid mating pili. Here, we report the cryo-EM structure of the RP4 pilus at 2.75 Å resolution. Uniquely, this revealed that the cyclic TrbC pilin subunit is not lipidated; the only known example of a mating pilus made in the absence of phospholipids. This discovery challenges the prevailing model that the lipid moiety is essential for pili biogenesis and conjugation.

Bacterial conjugation [1], [2], an efficient mechanism of horizontal gene transfer playing a central role in the dissemination of antibiotic resistance, relies on extracellular appendages known as conjugative pili (mating pili); these dynamic filaments mediate intercellular contacts between donor and recipient bacteria and facilitate DNA transfer [3]. Studies of the archetypical F-pilus, encoded by the pOX38 and pED208 plasmids, provided detailed molecular insights into the pilus biogenesis process [4], [5], [6]. Briefly, the TraA pilin, which is synthesized as a pre-pilin, is cleaved in the cytosol by the signal peptide peptidase LepB before it is inserted into the inner membrane (IM), where it accumulates as a reservoir. While extracted from the IM the pilin co-extracts phospholipids. The pilin-phospholipid complex then polymerises into a helical filament on top of the type IV secretion system (T4SS), a multi-protein complex spanning the inner and outer membranes and mediating plasmid transfer [3],[4], [5], [6].

Structural studies of the pOX38/pED208/pKpQIL- (IncF) [4], R388- (IncW) [7], and pKM101- (IncN) [8] encoded pili revealed that they are hollow helical tubes, approximately 8-10 nm in diameter, with a central lumen of 2.5-3 nm, wide enough to accommodate the relaxase-bound single-stranded (ss) DNA [9]. The pilins are composed of three α-helices, α1-α3, connected by short loops; the helices display conformational variations in different pili. All known

conjugative bacterial pili, the archaeal import pili and the T-pilus encoded by the Ti-plasmid of *Agrobacterium tumefaciens* have a bound phospholipid (e.g. phosphatidylglycerol – PG, phosphatidylethanolamine – PE, phospholipid GDGT-0, phosphatidylcholine – PC, and C_{25}-C_{25}, C_{25}, C_{25} diether lipids) at a 1:1 stoichiometry with the pilin subunit. In the retractable F-pilus, the phospholipid acyl chains are parallelly arranged [4], while in the unretractable R388 pilus they are splayed [7]. Disrupting the interface between the PG and the pED208 TraA pilin by site directed mutagenesis aborted pilus biogenesis [4]. The phospholipids lining the pilus lumen have been suggested to neutralise its positive charge [4]. The exception is the T pilus where the PE contributes to the positive charge within the pilus lumen [10], [8].

We have recently reported a deviation from the prevailing model, showing that the TrhA pilin, encoded by the prototype IncHI1 plasmid R27, undergoes posttranslational C-terminal cleavage and cyclization [11]. Cyclization is mediated via an intramolecular covalent head-to-tail peptide bond between G1 and D69, forming a ring pilin structure. The cyclic pilin is lipidated and the overall pilus cryo-EM structure resembles the archetypical F-pilus [4]. Like the R27 ThrA pilin, it was previously shown biochemically that the RP4 (IncP) plasmid-encoded TrbC pilin is also cyclic [12], [13], [14].

Several studies provided detailed molecular insights into the RP4 pilus biogenesis process [12], [13], [14]. Following removal of the signal peptide by LepB, maturation of TrbC requires a yet unknown chromosome-encoded protease, cleaving the C-terminal 27 residues, and the plasmid-encoded TraF, which while cleaving four additional C-terminal residues cyclises TrbC by forming a peptide bond between S1 and G78 of the mature pilin [12], [13], [14]. Here, we report the cryo-EM structure of the RP4 pilus, which unexpectedly revealed that the cyclic TrbC pilin assembles into a pilus in the absence of phospholipids. This finding offers an alternative, lipid-independent pilus biogenesis pathway, that diverges from the canonical model.

66 We adopted a similar approach to express and purify the RP4 pilus for structural studies as we
67 reported for the H-pilus [11]. Briefly, RP4 pili were purified from *E. coli* MG1655 Δ*fimA* (lacking
68 expression of type I pili) using the needle-shaving and precipitation method (see Materials and
69 Methods) (Figure 1a). Using this method, we determined the cryo-EM structure of the RP4
70 pilus at 2.75 Å resolution (map:map FSC, 0.143 threshold) employing helical reconstruction in
71 cryoSPARC by imposing helical (rise 15.15 Å, twist 24.62°) and C5 symmetry (Figure 1b, c,
72 d). The outer diameter of the pilus is ~80 Å and the lumen diameter ~20 Å, comparable to other
73 conjugation pilus structures. The Coulomb map and structure confirm that the TrbC pilin is
74 cyclized as a result of condensation of the Ser1 amine and Gly78 carboxyl residue and agrees
75 with the previous biochemical studies [13] (Figure 1c). The TrbC pilin contains three α-helices,
76 α1-α3; the α1 and α2 helices are fused to form two α1/2 helices connected to a split α3 helix,
77 $\alpha3_1$ and $\alpha3_2$, through a connecting loop. This arrangement resembles the conformation of the
78 reported acyclic VirB2 pilin forming the T-pilus rather than the cyclic TrhA pilin forming the
79 H pilus that has a split α3 helix connected via a loop to α1 and α2 helices (Figure 2a). Although
80 the mature cyclic TrbC pilin has an additional 10 C-terminal residues compared to other pilins
81 (Figure 2a, b), the extra residues do not impact the overall structure and can be accommodated
82 by displacement of the $\alpha3_2$ helix by 5 degrees along Gly66 (Figure 2c).

83 Unexpectedly, the structure revealed that the TrbC pilin is not associated with a phospholipid.
84 Inspection of the maps did not reveal any lipid-like density in the proximity of the α2 or α3
85 helices where the bound lipids are usually located (Figure 1c, 1e, 2a). The lack of an associated
86 phospholipid is unexpected as all pilus structures reported to date have been shown to be
87 associated with IM lipids needed for biogenesis. In the lipidated pilins, the phospholipid
88 mediate contacts with neighbouring pilin subunits that provide extra stability in addition to the
89 intermolecular interactions (Figure 2c). The hydrophobic residues in TraA (pED208/F pilus)
90 and ThrA (R27/H pilus) interact with the lipid acyl chain (Figure 2c). In contrast, interactions

of the TrbC protomers are mediated primarily by intermolecular van der Waals forces (Figure 2c). In the absence of a bound phospholipid in the protomer interface, α3 and α2' from the next protomer, of the TrbC protomers come closer to 'fill-in' the space in the absence of a phospholipid via a tight α3 and α2' interface; this results in an offset of the two adjacent TrbC protomers by 24° rotation and 15 Å rigid body shift relative to the VirB2/ThrA protomers (Figure 2c). TrbC also makes extensive interactions with 6 surrounding subunits whereas in lipidated-pilus structures the associated phospholipids are found at the pilin interfaces (Figure 2c). The presence of different phospholipid headgroups facing the lumen of pili change their overall charge from electropositive towards to neutral/slight electronegative (Figure 1d, 1e). The lumen of the RP4 pilus is negatively charged. The presence of a PE lipid in the T-pilus lumen results in alternating positive to negative charge; this may be because the T pilus transports diverse range of substrates beyond DNA [10].

The distinct differences between pilus structures in bacteria (cyclic and acyclic) and archaea give fundamental insights into plasmid biology, pilus biogenesis, DNA transfer and evolution. It remains unclear why certain pili, acyclic or cyclic, such as the F- or H-pilus, adopt a 5-fold symmetry where others such as the pKpQIL pilus adopt a one-start helical symmetry [15]; this plasticity in pilus architecture underscores the emergence of adaptable bacterial conjugation systems throughout evolution. For pili that retract, such as the F-pilus, it has been suggested that phospholipids may (i) assist in the assembly and disassembly of pilin subunits from the filament by lowering the energetic cost, (ii) provide the pilus with mechanical flexibility encountered in natural environments and (iii) repel negatively charged DNA and facilitate relaxase-ssDNA transfer. It has been suggested that although the R388 pilus is lipidated, it does not retract because of the non-canonical binding of the phosphatidylglycerol at helix α3 with its acyl chains splayed; the phospholipid would have to undergo an energetically costly rearrangement for the pilus to retract [7]. The absence of bound phospholipids in RP4 pilus

explains its rigidity and why it is not retractable [16]. In conclusion, our data suggest that the phospholipid is not needed for TrbC extraction from the IM, pilus biogenesis and relaxase-ssDNA transfer. Taken together, our finding of phospholipid-independent biogenesis redefines the role of phospolipids in conjugation pilus biogenesis and DNA transfer.

Acknowledgements

We thank Prof Christopher Thomas, University of Birmingham, for providing us with the IncP plasmid. We would like to thank Prof Edward Egelman, University of Virginia, for critical reading of the manuscript. We would like to acknowledge Diamond for access and support of the cryo-EM facilities at the UK national electron Bio-Imaging Centre (eBIC) under visit BI33230. This project made use the Computing Platform for Electron Microscopy at Imperial College funded by the BBSRC Mid-range equipment Initiative 22ALERT (BB/X019284/1). NI is funded by a Fellowship from The Naito Foundation.

Author contributions

KB and GF conceived and supervised the study. NI purified the RP4 pilus, determined the cryo-EM structure and performed model building and refinement. NI, GF and KB analyzed the structures. NI, GF and KB wrote the manuscript.

Competing interests

The authors declare no competing interests.

Materials and Methods

Expression and purification of RP4 pilus

The RP4 pilus was purified following the protocol used to prepare the H pilus [11]. Briefy, bacterial cells from an overnight culture were shaved through 25 G needles 25~30 times and were centrifuged at 50,000 xg for 1 h. The pilus filaments were precipitated using PEG 6,000 at a final concentration of 5% with stirring for 1 h, which was followed by centrifugation at 50,000 xg for 30 min. The supernatant was removed, and the pellet was resuspended in 200 µL imaging buffer (50 mM Tris-HCL pH 8, 200 mM NaCl). The solution containing the filaments was dialyzed overnight in imaging buffer. Sample purity was judged by SDS-PAGE.

Grid preparation and cryo-EM data collection

For grid preparation, 3 µL of the purified sample at ~4 mg/mL was applied to a glow-discharged carbon grid (Quantifoil R1.2/1.3, Cu, 300 mesh). The grid was blotted with a blotting force of 0 for 3 sec at 4°C and 100% humidity, and flash-frozen in liquid ethane using a Vitrobot Mark IV (Thermo Fisher Scientific). Cryo-EM data were collected on 300 kV Titan Krios G2 (Thermo Fisher Scientific) with a Falcon 4i detector and Selectris X energy filter at the Electron Bioimaging Center (eBIC), UK. A total of 3,405 movies were collected at a magnification of ×130,000 (pixel size of 0.921 Å/pixel) with a total electron dose of 50 e/Å2. The defocus range was set between -0.8 and -1.8 µm. All data were automatically acquired using EPU software. The data collection parameters are summarized in Supplementary Table 1.

Cryo-EM Data Processing and Model Building

The collected data were processed using cryoSPARC (v.4.6.1) [17]. Data were collected from a Titan Glacios and Krios, analyzed separately, and 2D images and initial volume from Glacios dataset were used for initial reconstruction. Both datasets were processed following similar

steps. Motion correction was performed using Patch Motion Correction, and CTF estimation for micrographs was done by Patch CTF estimation [17]. Particles from the Glacios dataset were manually picked from all micrographs and extracted in a binned state at 2.76 Å/pix. The extracted particles were classified in two rounds in 2D classification, and selected high-quality particles were used as references for the Filament tracer. Three rounds of 2D classification from the whole dataset was used to select particles for helical reconstruction. Helical symmetry search job suggested an axial rise of ~15.3 Å and a twist of ~24.6º, along with 5-fold point group symmetry. These symmetry parameters were used as starting parameters for helical reconstruction using Helix refine. 4.0 Å P-pilus map was reconstructed from Glacios data set. Then, 2D references and 3D model were used for reference to Krios dataset. In Krios dataset, 3,405 movies were collected. After Motion Correction and CTF refinement, template pick was performed with Filament tracer using a 2D reference from the Glacios dataset. 4,302,764 particles were extracted in the binning state. Three rounds of 2D classification were performed, and 10,792 particles were selected. Using 3D volume and helical parameters from the Glacios dataset, Helical refinement, local CTF refinement and Reference-based motion correction were performed several times. The final RP4 pilus helical reconstruction showed 2.75 Å resolution using 10,729 particles, with a rise of 15.15 Å and a twist of 24.62°.

Ab initio model building and real space refinement were performed in PHENIX [18], [19]. The model was subjected to iterative cycles of refinement and manual rebuilding in COOT [20]. The structural model was validated using MolProbity [21]. The processing parameters and refinement statistics are summarized in Supplementary Table 1.

Data availability

The cryo-EM maps have been deposited in the Electron Microscopy Data Bank (EMDB) under accession code EMD-65024. The structural coordinates have been deposited to the RCSB Protein Data Bank (PDB) under the accession code 9VF4. Raw images were submitted to the Electron Microscopy Public Image Archive (EMPIAR) with ID EMPIAR-XXXX.

Figure Legends

Figure 1. Cryo-EM structure of the RP4 pilus. (a) Micrograph of the straight and rigid RP4 pilus. (b) Cryo-EM map of RP4-pilus. One right-handed 5-start strand is shown in green and the rest of the filament in grey. The pilus has an outer diameter of ~80 Å and an inner lumen diameter of ~20 Å. (c) Atomic model of the RP4 pilus (left panel). The TrbC pilin is cyclic and lacks a bound phospholipid as revealed by the Coulomb map. The site of cyclization is indicated by an arrowhead and the residues in orange. (d) The F-pilus lumen is lined by PG (indicated by red sticks) compared to the RP4 pilus. (e) The RP4 pilus lumen displays a strong electronegative charge compared to the other bacterial pili that appear more neutral, whereas the T pilus has an alternating positive and negative charge. The exterior of the different pili displays variable charge profile.

Figure 2. Comparison of the TrbC with other conjugative pilins. (a) The conformation of TrbC pilin resembles the VirB2. Pilins of different conjugative pili bind diverse phosholipids and in different conformation. The pilin structures and their associated lipids are shown in cartoon and sticks, respectively. (b) The C-terminal 27 residues of the pre-TrbC pilin are cleaved by an unknown chromosomal protease (highlighted in grey) and is further processed by TraF-mediated cleavage of 4 additional residues (highlighted in yellow), linked to cyclisation. The C-terminus of the F- and T-pilus that is not processed. Cyclization of the R27 ThrA pilin involves cleavage of the last 5 residues (highlighted in yellow). (c) In the absence of phospholipids, the neighbouring TrbC protomers occupy the empty lipid-space to make extensive stabilizing interactions (top row) compared to the lipidated ThrA (bottom row). Each pilin protomer is shown in either surface or cartoon representation and colored differently.

References

1 Low, W. W. *et al.* Mating pair stabilization mediates bacterial conjugation species specificity. *Nat Microbiol* **7**, 1016-1027 (2022). https://doi.org/10.1038/s41564-022-01146-4

2 Frankel, G. *et al.* Plasmids pick a bacterial partner before committing to conjugation. *Nucleic Acids Res* **51**, 8925-8933 (2023). https://doi.org/10.1093/nar/gkad678

3 Waksman, G. From conjugation to T4S systems in Gram-negative bacteria: a mechanistic biology perspective. *EMBO Rep* **20** (2019). https://doi.org/10.15252/embr.201847012

4 Costa, T. R. D. *et al.* Structure of the Bacterial Sex F Pilus Reveals an Assembly of a Stoichiometric Protein-Phospholipid Complex. *Cell* **166**, 1436-1444 e1410 (2016). https://doi.org/10.1016/j.cell.2016.08.025

5 Mace, K. *et al.* Cryo-EM structure of a type IV secretion system. *Nature* **607**, 191-196 (2022). https://doi.org/10.1038/s41586-022-04859-y

6 Hu, B., Khara, P. & Christie, P. J. Structural bases for F plasmid conjugation and F pilus biogenesis in Escherichia coli. *Proc Natl Acad Sci U S A* **116**, 14222-14227 (2019). https://doi.org/10.1073/pnas.1904428116

7 Vadakkepat, A. K. *et al.* Cryo-EM structure of the R388 plasmid conjugative pilus reveals a helical polymer characterized by an unusual pilin/phospholipid binary complex. *Structure* **32**, 1335-1347 e1335 (2024). https://doi.org/10.1016/j.str.2024.06.009

8 Amro, J. *et al.* Cryo-EM structure of the Agrobacterium tumefaciens T-pilus reveals the importance of positive charges in the lumen. *Structure* **31**, 375-384 e374 (2023). https://doi.org/10.1016/j.str.2022.11.007

9 Williams, S. M. *et al.* Cryo-EM Structure of the relaxosome, a complex essential for bacterial mating and the spread of antibiotic resistance genes. *Nat Commun* **16**, 4906 (2025). https://doi.org/10.1038/s41467-025-60116-6

10 Beltran, L. C. *et al.* Archaeal DNA-import apparatus is homologous to bacterial conjugation machinery. *Nat Commun* **14**, 666 (2023). https://doi.org/10.1038/s41467-023-36349-8

11 Ishimoto, N. *et al.* Cryo-EM structure of the conjugation H-pilus reveals the cyclic nature of the TrhA pilin. *Proc Natl Acad Sci U S A* **122**, e2427228122 (2025). https://doi.org/10.1073/pnas.2427228122

12 Haase, J. & Lanka, E. A specific protease encoded by the conjugative DNA transfer systems of IncP and Ti plasmids is essential for pilus synthesis. *J Bacteriol* **179**, 5728-5735 (1997). https://doi.org/10.1128/jb.179.18.5728-5735.1997

13 Eisenbrandt, R. *et al.* Conjugative pili of IncP plasmids, and the Ti plasmid T pilus are composed of cyclic subunits. *J Biol Chem* **274**, 22548-22555 (1999). https://doi.org/10.1074/jbc.274.32.22548

14 Eisenbrandt, R., Kalkum, M., Lurz, R. & Lanka, E. Maturation of IncP pilin precursors resembles the catalytic Dyad-like mechanism of leader peptidases. *J Bacteriol* **182**, 6751-6761 (2000). https://doi.org/10.1128/JB.182.23.6751-6761.2000

15 Zheng, W. *et al.* Cryoelectron-Microscopic Structure of the pKpQIL Conjugative Pili from Carbapenem-Resistant Klebsiella pneumoniae. *Structure* **28**, 1321-1328 e1322 (2020). https://doi.org/10.1016/j.str.2020.08.010

16 Samuels, A. L., Lanka, E. & Davies, J. E. Conjugative junctions in RP4-mediated mating of Escherichia coli. *J Bacteriol* **182**, 2709-2715 (2000). https://doi.org/10.1128/JB.182.10.2709-2715.2000

17 Punjani, A., Rubinstein, J. L., Fleet, D. J. & Brubaker, M. A. cryoSPARC: algorithms for rapid unsupervised cryo-EM structure determination. *Nat Methods* **14**, 290-296 (2017). https://doi.org/10.1038/nmeth.4169

18 Adams, P. D. *et al.* PHENIX: a comprehensive Python-based system for macromolecular structure solution. *Acta crystallographica. Section D, Biological crystallography* **66**, 213-221 (2010). https://doi.org/10.1107/S0907444909052925

19 Afonine, P. V. *et al.* Real-space refinement in PHENIX for cryo-EM and crystallography. *Acta Crystallogr D Struct Biol* **74**, 531-544 (2018). https://doi.org/10.1107/S2059798318006551

20 Emsley, P. & Cowtan, K. Coot: model-building tools for molecular graphics. *Acta Crystallogr D Biol Crystallogr* **60**, 2126-2132 (2004).

21 Chen, V. B. *et al.* MolProbity: all-atom structure validation for macromolecular crystallography. *Acta crystallographica. Section D, Biological crystallography* **66**, 12-21 (2010). https://doi.org/10.1107/S0907444909042073

Figure 1.

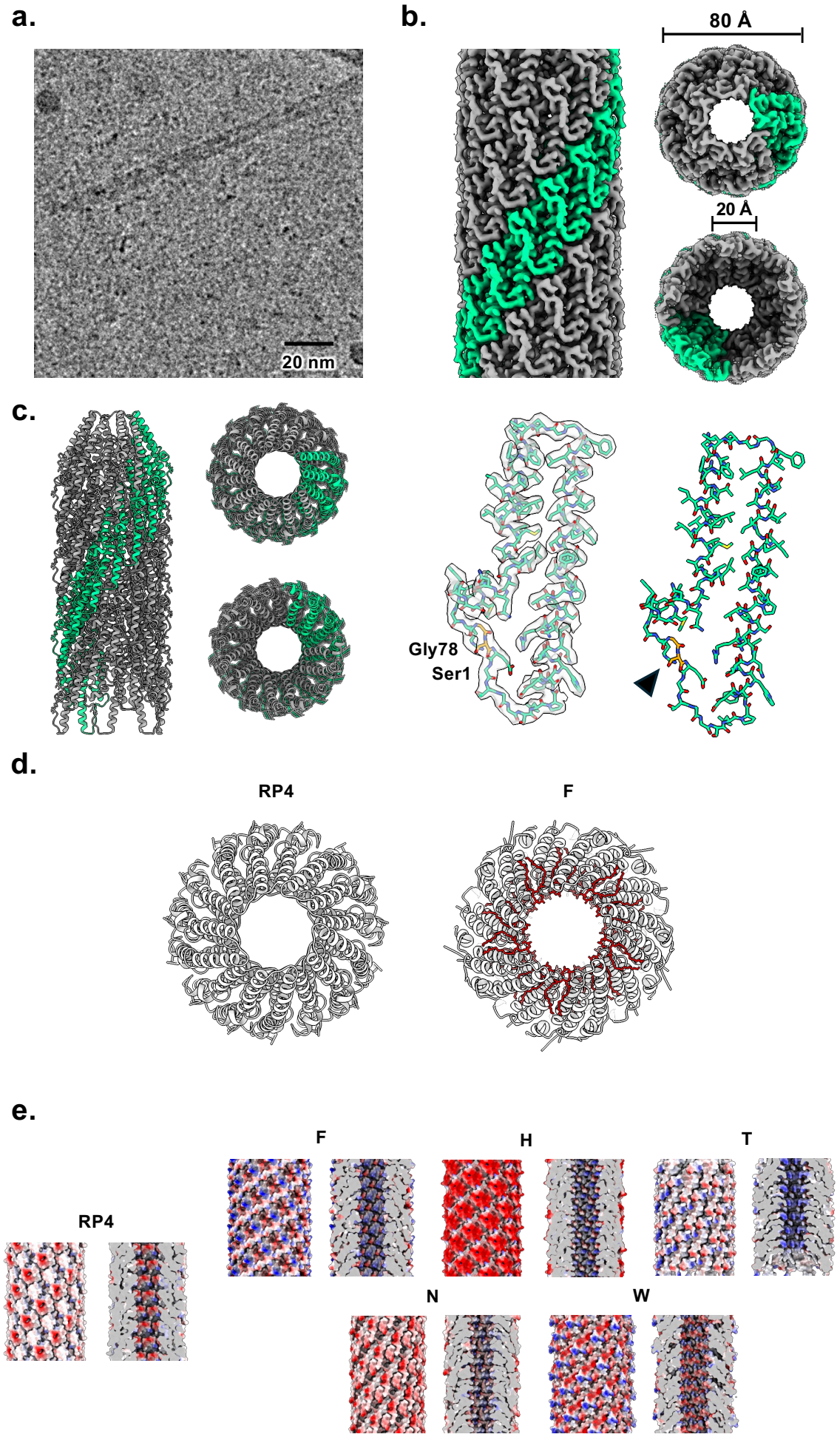

Figure 2.

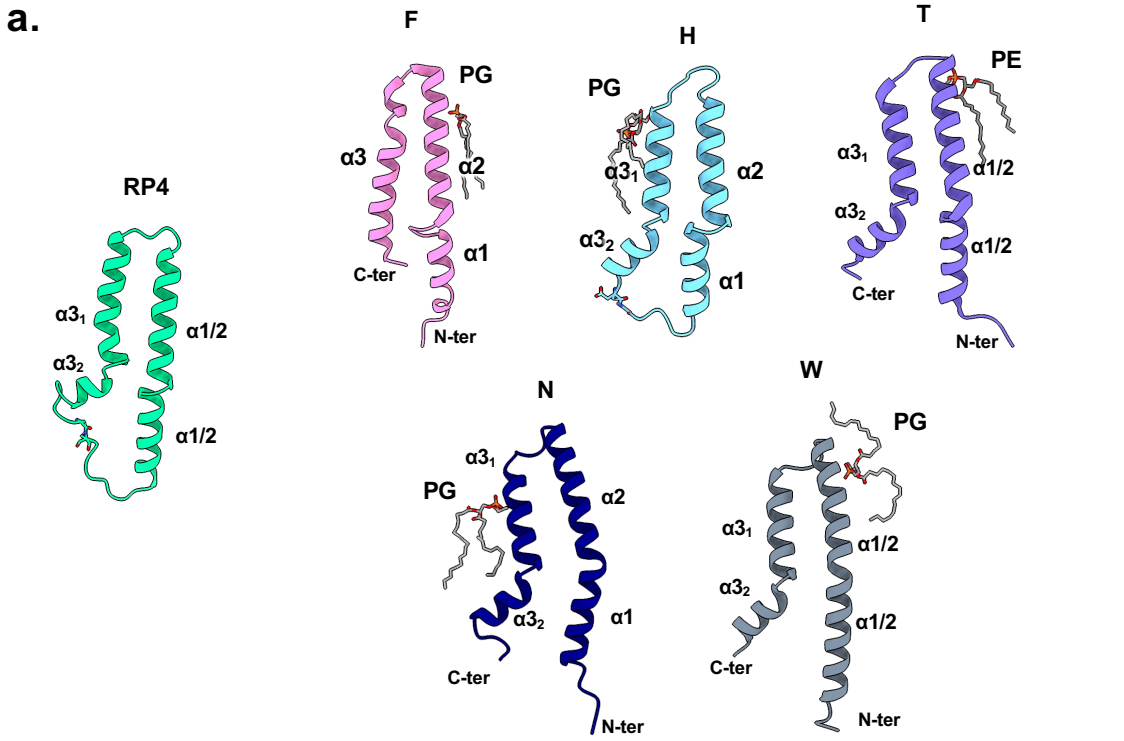
a.
RP4
α3₁
α3₂
α1/2
α1/2
F
PG
α3
α2
α1
C-ter
N-ter
H
PG
α3₁
α2
α3₂
α1
T
PE
α3₁
α1/2
α3₂
α1/2
C-ter
N-ter
N
α3₁
PG
α2
α3₂
α1
C-ter
N-ter
W
PG
α3₁
α1/2
α3₂
α1/2
C-ter
N-ter

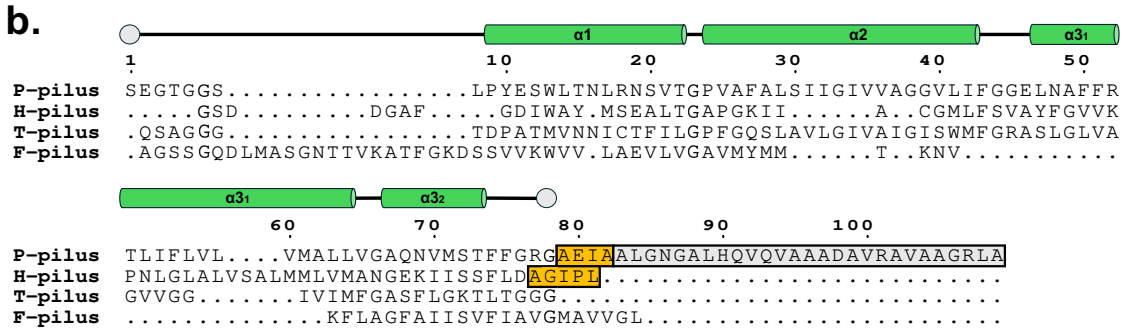
b.
α1
α2
α3₁
1 10 20 30 40 50
P-pilus SEGTGGS.....LPYESWLTNLRNSVTGPVAFALSIIGIVVAGGVLIFGGELNAFFR
H-pilus .....GSD.....DGAF.....GDIWAY.MSEALTGAPGKII.....A..CGMLFSVAYFGVVK
T-pilus .QSAGGG.....TDPATMVNNICTFILGPFGQSLAVLGIVAIGISWMFGRASLGLVA
F-pilus .AGSSGQDLMASGNTTVKATFGKDSSVVKWVV.LAEVLVGAVMYMM.....T..KNV.....
α3₁
α3₂
60 70 80 90 100
P-pilus TLIFLVL....VMALLVGAQNVMSTFFGRGAEIAALGNGALHQVQVAAADAVRAVAAGRLA
H-pilus PNLGLALVSALMMLVMANGEKIISSFLDAGIPL.....
T-pilus GVVGG.....IVIMFGASFLGKTLTGGG.....
F-pilus .....KFLAGFAIISVFIAVGMAVVGL.....

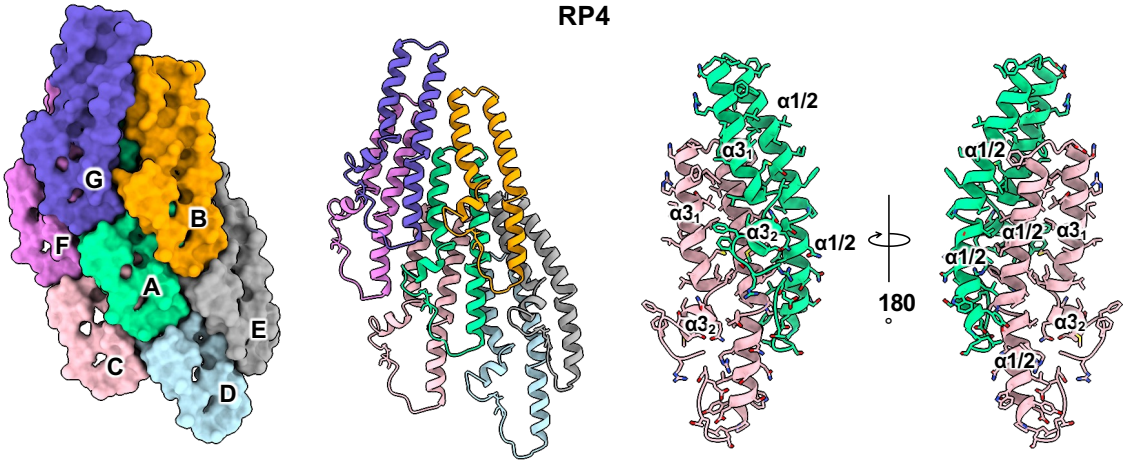
c.
RP4
G
B
F
A
E
C
D
α1/2
α3₁
α3₁
α3₂
α1/2
α3₂
180
α1/2
α1/2
α3₁
α1/2
α3₂
α1/2

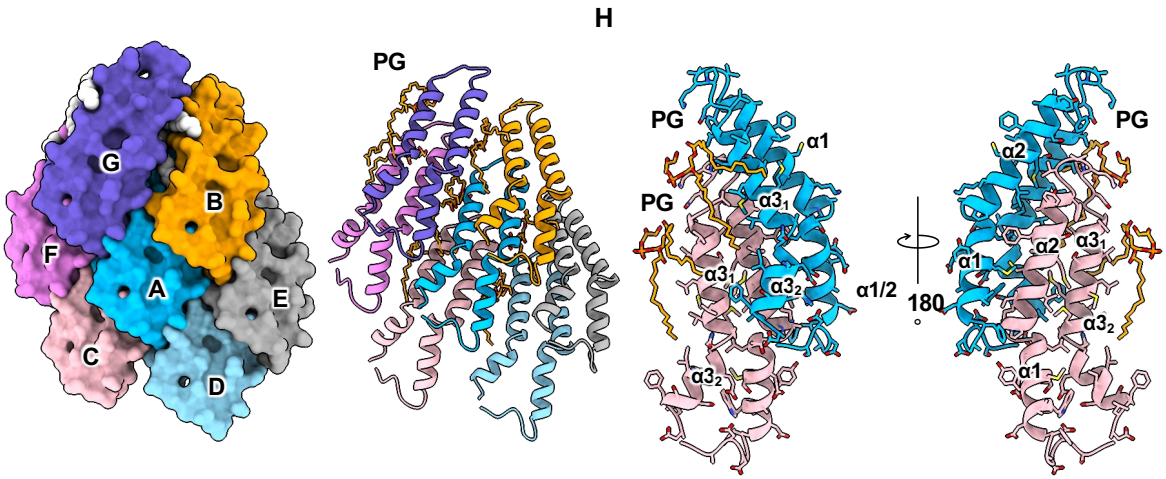
H
PG
G
B
F
A
E
C
D
PG
PG
α1
α3₁
α3₁
α3₂
α1/2
α3₂
180
PG
α2
α1
α2
α3₁
α3₂
α1